Active fault-tolerant control of rotation angle sensor in steer-by-wire system based on multi-objective constraint fault estimator

Qinjie Yang, Guozhe Shen and Chao Liu
School of Automotive Engineering, Dalian University of Technology, Dalian, China
Zheng Wang
Institute of Industrial Science, The University of Tokyo, Tokyo, Japan
Kai Zheng
Marine Electrical Engineering College, Dalian Maritime University, Dalian, China, and
Rencheng Zheng
Key Laboratory of Mechanism Theory and Equipment Design, Ministry of Education, Tianjin University, Tianjin, China

Abstract

Purpose – Steer-by-wire (SBW) system mainly relies on sensors, controllers and motors to replace the traditionally mechanical transmission mechanism to realize steering functions. However, the sensors in the SBW system are particularly vulnerable to external influences, which can cause systemic faults, leading to poor steering performance and even system instability. Therefore, this paper aims to adopt a fault-tolerant control method to solve the safety problem of the SBW system caused by sensors failure.

Design/methodology/approach – This paper proposes an active fault-tolerant control framework to deal with sensors failure in the SBW system by hierarchically introducing fault observer, fault estimator, fault reconstructor. Firstly, the fault observer is used to obtain the observation output of the SBW system and then obtain the residual between the observation output and the SBW system output. And then judge whether the SBW system fails according to the residual. Secondly, dependent on the residual obtained by the fault observer, a fault estimator is designed using bounded real lemma and regional pole configuration to estimate the amplitude and time-varying characteristics of the faulty sensor. Eventually, a fault reconstructor is designed based on the estimation value of sensors fault obtained by the fault estimator and SBW system output to tolerate the faulty sensor.

Findings – The numerical analysis shows that the fault observer can be rapidly activated to detect the fault while the sensors fault occurs. Moreover, the estimation accuracy of the fault estimator can reach to 98%, and the fault reconstructor can make the faulty SBW system to retain the steering characteristics, comparing to those of the fault-free SBW system. In addition, it was verified for the feasibility and effectiveness of the proposed control framework.

Research limitations/implications – As the SBW fault diagnosis and fault-tolerant control in this paper only carry out numerical simulation research on sensors faults in matrix and laboratory/Simulink, the subsequent hardware in the loop test is needed for further verification.

Originality/value – Aiming at the SBW system with parameter perturbation and sensors failure, this paper proposes an active fault-tolerant control framework, which integrates fault observer, fault estimator and fault reconstructor so that the steering performance of SBW system with sensors faults is basically consistent with that of the fault-free SBW system.

Keywords Active fault-tolerant control, Fault estimation, Sensors failure, Steer-by-wire

Paper type Research paper

1. Introduction

The steer-by-wire (SBW) is originated from the fly-by-wire system in the airplane (Waraus, 2009), which is different from the traditional steering system. The SBW system uses control signals to replace the traditional mechanical connection between the steering wheel and the road wheel, only relying on sensors,

The current issue and full text archive of this journal is available on Emerald Insight at: **https://www.emerald.com/insight/2399-9802.htm**

Journal of Intelligent and Connected Vehicles
4/1 (2021) 1–15
Emerald Publishing Limited [ISSN 2399-9802]
[DOI 10.1108/JICV-08-2020-0007]

This study was supported in part by the State Key Laboratory of Automotive Safety and Energy under Project No. KF1815, and the National Natural Science Foundation of China (No. 52071047 and No. 51975089).

Received 3 August 2020
Revised 26 October 2020
Accepted 7 November 2020

motors and controllers to achieve steering. This new technology completely gets rid of the limitations of the traditional steering system by brings many significant benefits, such as setting a variable transmission ratio to reduce the driving burden, increasing the safety of the collision and improving vehicle stability and mobility (Mi *et al.*, 2018). The SBW system usually uses the measurement output of the sensors as a feedback signal to control vehicle gestures, but the sensors are vulnerable to unexpected changes in external surroundings, resulting in stuck, gain, deviation and signal interruption (Gao *et al.*, 2017). This will cause the SBW controller to generate wrong control commands, so the performance of the attitude control system will be degraded and the steering system will be unstable resulting in driving safety problems.

On the one hand, to ensure the security of the SBW system, a hardware redundancy can be used as a backup system. In other words, the SBW system uses conventional mechanical steering linkage, multiple sensors, multiple microprocessors and multiple actuators to ensure safety, such as Infiniti Q50, General Motors' Hy-wire, Danfoss original equipment manufactures and Delphi's four-wheel steering vehicle. However, the backup system is more expensive, not only increasing the weight of the vehicle but also increasing the complexity and development cost of the SBW system.

On the other hand, a software redundancy can be adopted, that the fault-tolerant control method can be used to solve the security problem of the SBW system, which can not only reduce the total number of redundant hardware components and the cost of system development but also to ensure the overall security and steering performance of the SBW system (Ito and Yoshikazu, 2013).

In recent years, many scholars have studied the fault detection (FD) theory based on the mathematical model of the SBW system (Anwar and Niu, 2010; Tian *et al.*, 2009; Zhang and Zhao, 2016; Chengwei *et al.*, 2010; Lu *et al.*, 2017). Its core idea is to construct residual by using the SBW system and designed observer, and then use some decision rules to judge the occurrence of faults. However, the FD based on the mathematical model adopts an accurate SBW mathematical model. These FD methods are always inaccurate in the presence of parameter variations in the SBW system, such as variation of the tire cornering stiffness and the system damping coefficient. To resolve this problem, sliding mode control (Huang *et al.*, 2017; Dhahri *et al.*, 2012) can be used to design the fault observer or the $H\_/H\infty$ index (Chen and Patton, 2017; Aouaouda *et al.*, 2015; Hou and Patton, 1996; Zhou *et al.*, 2017; Yang *et al.*, 2013; Chilali and Gahinet, 1996) can be used to design the fault observer, to ensure that the FD is robust to influence of interference. However, although the fault observer designed in these previous studies can detect system failure, it is still difficult to determine faulty components and identify the fault size and time-varying characteristics.

As an indispensable part of fault diagnosis, fault estimation has attracted more and more attention because of its ability to determine the time when the fault occurred, the size and time-varying characteristics of the fault and its superiority in reducing system redundancy. Extensive investigations have been conducted on sensors faults estimation in satellite control systems and flight control systems (Zhang *et al.*, 2013; Olfa *et al.*, 2015; Liang *et al.*, 2019; Wenhan *et al.*, 2020). In Xiao *et al.* (2019), an adaptive observer is proposed for the simultaneous actuator and sensor faults in aircraft engines, and a fault-tolerant control system is designed on this basis of the adaptive observer. In Yang *et al.* (2015), the problem is studied about sensors faults estimation, actuator FD and isolation for a class of uncertain non-linear systems. However, the existing conditions of the fault estimation observer are not given in these articles, which makes it difficult to judge whether the fault estimation observer to be designed is suitable for the controlled system. Second, the fault estimation algorithm used in these articles is based on the output error between the adaptive observer and the system. The generated output error includes the fault estimation error and the state estimation error. There is a coupling between the fault estimation error and the output error so that the designed fault estimation algorithm cannot take into account the accuracy and speed of the fault estimation. Therefore, it is necessary to further suppress the impact of system uncertainty on the fault estimation, to improve the transient performance of the fault estimation. In addition, previous research studies had few mentioned the problem of sensors faults estimation in SBW system. Inspired by this sensors faults estimation method, and at the same time, to overcome the difficulties and deficiencies in the above designs, this study proposed a multi-objective constrained fault estimator (MCFE) based on residual information, so that the fault value from the fault estimator can be identical to the actual fault value, and gives the existing condition of the fault estimator.

In addition, apart from FD and estimation in the event of a component failure in the SBW system, fault reconstruction is of great significance to make the car run smoothly as soon as possible in such a hazardous situation. In Mortazavizadeh *et al.* (2020), a novel FD, isolation and reconstruction control technique was proposed for the failure of voltage and current sensors in the SBW system, in which the problem of simultaneous failure of voltage and current sensors could not be solved. A comprehensive method of reconfigurable fault-tolerant control system for SBW vehicles is proposed in Wada *et al.* (2013). However, the system has actuator redundancy, which will increase system development costs. Huang *et al.* (2018) adopt the minimax model predictive control (MPC) in the delta-domain to realize the tracking performance under actuator fault, system uncertainties and disturbance. However, the MPC controller is lacking in solving the problem of the actuator, which makes the system in an unstable state.

In view of the above motivations, this paper proposes an active fault-tolerant control framework for the SBW system subject to sensors failure by introducing sensors fault detection, estimation and reconstruction techniques so as to realize higher-level safety performance. The main contributions of this paper can be marked as follows:

- A hierarchical fail-safe control framework is presented for cooperating detection, estimation, reconstruction, by which the higher-level safety performance of the SBW system subject to sensors failure is effectively assured. So the fault estimator can not only make up for the shortcomings of the fault observer but also the combination can give full play to their respective advantages.
- Different from the previous algorithms related to sensors faults estimation, the designed algorithm in this study achieves the decoupling of the fault estimation error and the output error between the fault estimator and the SBW

system, and the application of regional pole configuration can improve the transient performance of the fault estimation.

The rest of this paper is mainly organized as: an active fault-tolerant control problem for SBW system is described in Section 2, the SBW model with parameter perturbation and sensors failure is developed in Section 3, the fault tolerance control framework is proposed based on MCFE in Section 4 and the numerical analyzes are processed to validate the accuracy of fault estimation and effectiveness of the presented control framework in Section 5. Finally, the research is concluded in Section 6.

2. Problem description

As shown in Figure 1, it assumed that the rotation angle sensor, the yaw rate sensor and the lateral acceleration sensor in the steering module have a sudden failure due to changes in the external environment. Normally, the SBW system uses the measurement output of the sensor as a feedback signal to control the attitude of the vehicle; thereby, if the sensor fails, it will cause system instability and even cause traffic accidents. In addition, due to component manufacturing and measuring errors, it is difficult to obtain accurate SBW parameter values in practice. In addition, it is often difficult to accurately determine the cornering stiffness of a tire during driving. The changes in the above parameters will have a certain impact on the performance of the SBW system. Therefore, this paper also considers the perturbation of parameters equivalent to the damping coefficient of the front wheel and steering mechanism on the steering shaft, the damping coefficient of the motor shaft and the front wheel deflection stiffness.

The active fault-tolerant control framework contains three parts under the problem setting, namely, FD, fault estimation and fault reconstruction. First, a fault observer is designed to detect whether the system is faulty in real time, and if a fault occurs, it warns the driver and starts fault tolerance control. Then, a multi-objective fault estimator based on residual information obtained by the fault observer is designed to estimate the fault size of the sensors. Finally, the fault estimation value of the sensors and the fault output of the sensors are used for active fault-tolerance control.

Figure 1 Illustration of the SBW system with sensors failure

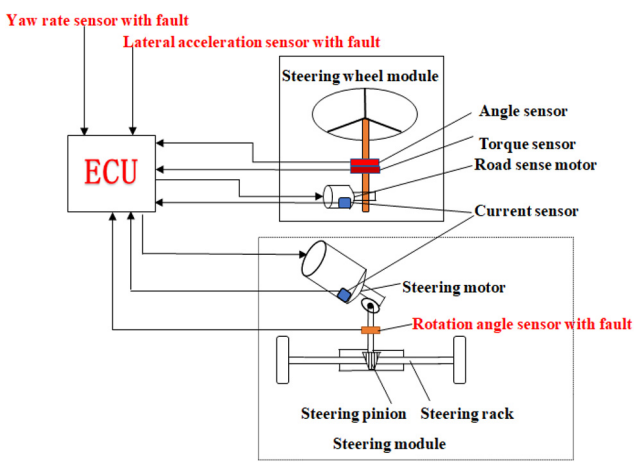

3. Modeling analysis

3.1 Vehicle model

In the driving procedure, the lateral stiffness, used to characterize the interaction between the tire and the road surface, is susceptible to changes in tire inflation pressure, road surface and weather conditions and it is often difficult to determine accurately. This paper assumes that the uncertainty of the cornering stiffness of the front wheel is ΔK_f, and establishes a linear two-degree-of-freedom vehicle model with parameter perturbation, as shown in Figure 2.

The equation of motion can be presented as:

$$\begin{cases} \dot{\beta} = -\dfrac{(K_f + \Delta K_f) + K_r}{mv_x}\beta + \dfrac{bK_r - a.(K_f + \Delta K_f)}{mv_x^2}\omega_r - \omega_r + \dfrac{(K_f + \Delta K_f)}{mv_x}\delta_f \\ \dot{\omega}_r = \dfrac{bK_r - a.(K_f + \Delta K_f)}{I_z}\beta - \dfrac{b^2K_r + a^2(K_f + \Delta K_f)}{I_z v_x}\omega_r + \dfrac{a.(K_f + \Delta K_f)}{I_z}\delta_f \end{cases} \tag{1}$$

where K_f and K_r are the cornering stiffness of the front and rear tires, respectively. β is the slip angle of the mass center. ω_r is the yaw angle speed. a and b are the distance from the front and rear axis to mass center, respectively. I_z is the rotary inertia of the vehicle body around z-axis. v_x is the vehicle longitudinal speed and m is the full-vehicle mass.

3.2 Systematic modeling

According to Figure 1, the structure of the SBW system mainly consists of three parts, namely, the steering wheel module, the steering module and the electronic control unit. The steering wheel module mainly transmits the driving intention of drivers and feeds back the road sense. The main hardware includes a road sense analog motor, rotation angle sensor, current sensor, torque sensor, traditional steering wheel and steering column.

The electronic control unit mainly implements three functions, namely, controlling the road sense analog motor to generate the road feel, controlling the steering execution motor to generate the steering torque and the fault-tolerant control of the main components of the entire system. This research focuses on the steering module, as shown in Figure 3, which mainly realizes the steering of the vehicle. It is based on the steering column assisted EPS, and the main hardware includes the steering execution motor, rotation angle sensor, current sensor, rack displacement sensor and traditional gear rack steering.

The current articles on SBW system research are mainly based on an accurate SBW model; however, due to the

Figure 2 Linear 2-DOF vehicle model with parameter perturbation

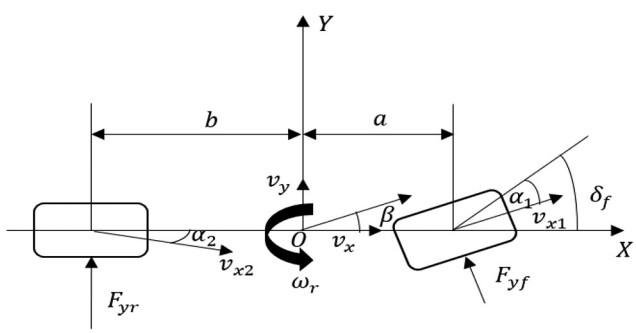

Figure 3 Structure diagram of steering module

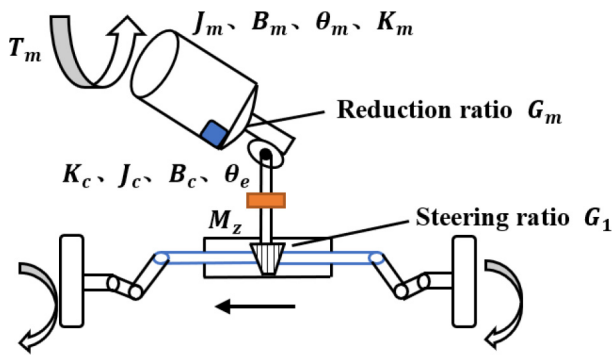

existence of component manufacturing and measurement errors, it is difficult to obtain accurate parameter value in practice. In addition, some parameters of SBW will also change because of environmental changes. Uncertain changes in the above parameters will have a certain impact on the performance of the SBW system. Therefore, this paper considers the parameter perturbation equivalent to the damping coefficients of the front wheels and steering mechanism on the steering shaft, and the damping coefficient of the motor shaft, and their uncertainties are ΔB_m and ΔB_c, respectively.

Taking the steering motor as the research objective, the dynamic equation can be obtained according to newton's law as follows:

$$\begin{cases} T_m = \mathfrak{J}_m \ddot{\theta}_m + (B_m + \Delta B_m)\dot{\theta}_m + T_a \\ T_a = K_m(\theta_m - G_m\theta_e) \\ T_m = K_t I_m \\ U = L\dot{I}_m + RI_m + K_e\dot{\theta}_m \end{cases} \tag{2}$$

where θ_m, $\mathfrak{J}_m$, B_m and K_m separately denote the angular position, moment inertia, viscous damping and shaft stiffness of the steering motor. G_m is the motor speed-reducing device transmission ratio. T_m and T_a are the power motor torque and the assist torque acting on the steering gear pinion, respectively. K_t and K_e are motor torque constant and counter electromotive force constant, respectively. L, R and I_m are the inductance, resistance and current of motor armature winding, respectively. U is the terminal voltage of the power motor.

Taking rack and front wheel steering components as the research object, the dynamic equation is as follows:

$$\mathfrak{J}_c\ddot{\theta}_c + (B_c + \Delta B_c)\dot{\theta}_c = GT_a + M_z, \tag{3}$$

where $\mathfrak{J}_c$ is the moment of inertia equivalent to the steering shaft of the front tire and steering mechanism. B_c is a viscous friction coefficient equivalent to the steering shaft of the steering mechanism and the front wheel. θ_c is the rotation angle sensor of the pinion shaft and M_z is the tire aligning torque.

Assuming that the front wheel slip angle is less than five degrees, the tire aligning torque M_z can be estimated using the following formula (Wenhan *et al.*, 2020),

$$\begin{cases} M_z = (t_p + t_m)F_{yf} = K_f\left(\beta + \dfrac{a\omega_r}{v_x} - \delta_f\right).(t_p + t_m) \\ \delta_f = \theta_c/i \end{cases}, \tag{4}$$

where t_p is the pneumatic trail. t_m is the mechanical trail. δ_f is the steering angle and i is the steering ratio.

The SBW system usually uses the measuring output of the sensor as a feedback signal to control the vehicle attitude; however, the rotation angle sensor, the yaw rate sensor and the lateral acceleration sensor will be suddenly failure due to the increase of the use cycle and the influence of external factors. Assuming that the sensors will continue to output measurement data at this time, but these data are not accurate. These data are specifically expressed as multiples of the correct data, some fixed value difference from the correct data, constant value and zero value. When the j (j = 1, 2, 3) sensors in the SBW system has a sudden failure, the corresponding measurement output can be expressed as:

$$y_{jf} = \Delta_j y_j + \alpha_j = y_j + (\Delta_j - 1)y_j + \alpha_j = y_j + f_{sj}, \tag{5}$$

where y_{jf} is the fault output of j (j = 1, 2, 3) sensor. y_j is the actual output. Δ_j is the fault gain and α_j is the fault constant deviation or lock value. Specially, $\Delta_j = 0$ and $\alpha_j = 0$ indicate that the sensor signal is interrupt.

While $f_{jf} = (\Delta_j - 1)\, y_j + \alpha_j$, combining with equation (1) ~ equation (5) and choosing the state vector $x(t) = \begin{bmatrix} \beta & \omega_r & \theta_m & \dot{\theta}_m & I_m & \theta_c & \dot{\theta}_c \end{bmatrix}^T$, control input vector $(t) = [U]$ and measurement output vector $y(t) = \begin{bmatrix} \beta & \omega_r & a_y & I_m & \theta_c \end{bmatrix}^T$ to establish SBW system model with parameter perturbation, sensors failure can be expressed as:

$$\begin{cases} \dot{x}(t) = (A + \Delta A)x(t) + Bu(t) \\ y_f(t) = Cx(t) + F_s f_s(t) \end{cases}, \tag{6}$$

where $F_s = \begin{bmatrix} F_s^1 & F_s^2 & F_s^3 \end{bmatrix}$ is the fault vector of yaw rate sensor, lateral acceleration sensor and rotation angle sensor, whose values are separately $F_s^1 = \begin{bmatrix} 0 & 1 & 0 & 0 & 0 \end{bmatrix}^T$, $F_s^2 = \begin{bmatrix} 0 & 0 & 1 & 0 & 0 \end{bmatrix}^T$ and $F_s^3 = \begin{bmatrix} 0 & 0 & 0 & 1 & 0 \end{bmatrix}^T$. fs = $[f_{s1}\ f_{s2}\ f_{s3}]$ is the fault values of yaw rate sensor, lateral acceleration sensor and rotation angle sensor, respectively.

This paper converts the uncertainty magnitude of the system model into additional interference, and combines it with the road information provided to the driver by the road surface to form system interference. Equation (6) can be rewritten as:

$$\begin{cases} \dot{x}(t) = Ax(t) + Bu(t) + Dd(t) \\ y_f(t) = Cx(t) + F_s f_s(t) \end{cases}, \tag{7}$$

where:

$$D = \begin{bmatrix} -\dfrac{1}{mv_x} & 0 & 0 \\ -\dfrac{a}{I_z} & 0 & 0 \\ 0 & 0 & 0 \\ 0 & -\dfrac{1}{\mathfrak{J}_m} & 0 \\ 0 & 0 & 0 \\ 0 & 0 & 0 \\ 0 & 0 & \dfrac{1}{\mathfrak{J}_c} \end{bmatrix} \quad d = \begin{bmatrix} \Delta K_f\left(\beta + \dfrac{a}{v_x}\omega_r - \dfrac{\theta_e}{G_1}\right) \\ \Delta B_m.\dot{\theta}_m \\ M_z - \Delta B_c.\dot{\theta}_e \end{bmatrix}.$$

Figure 4 Diagram of active fault-tolerant control framework

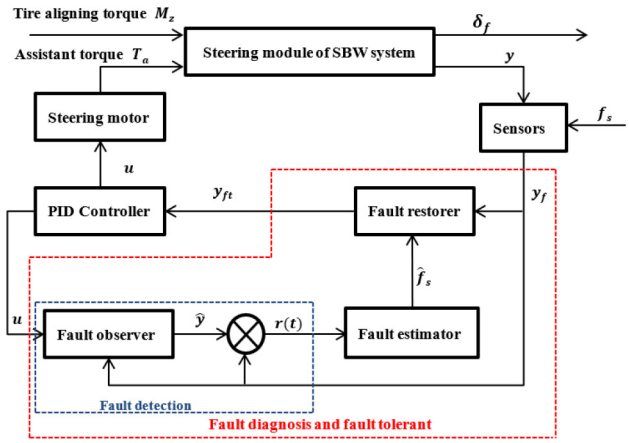

4. Active fault-tolerance control

As shown in Figure 4, the sensors fault tolerance control framework of the SBW system is mainly composed of a fault observer, a MCFE, and a fault reconstructor. The fault observer is used to obtain the residual between the observer and the SBW system, to determine whether the SBW system is faulty. The multi-objective constraint fault estimator uses the residual obtained by the fault observer to determine the size, time and time-varying characteristics of the faulty sensors. The reconstructor uses the values of fault estimation and the faulty sensor output in the SBW system, to achieve fault-tolerant control on the faulty sensor. In this way, the performance of SBW with sensors faults can still have the steering characteristics close to the fault-free SBW system, thereby achieving fault tolerance.

4.1 Fault observer design

In practical applications, SBW systems are often affected by system unmodeled dynamics and parameter changes. Therefore, when a fault occurs, it is necessary to design a multi-objective fault observer. On the one hand, the generated residual is sensitive to faults. Usually, the H_- index of the fault-to-residual transfer function $G_{r_f f}(s)$ is used to describe the sensitivity of residual to faults in the worst case.

On the other hand, the generated residual is robust to disturbance, and the robust performance of residual to disturbance is usually characterized by the H_∞ norm of the transfer function $G_{r_d d}(s)$. Therefore, the structure of the fault observer is shown in Figure 5. Its design is the process of solving the feedback gain matrix L. After L is obtained, the residual can be obtained and the residual can be compared with the set threshold to judge whether the system has a sensor fault.

According to the above figure, the following equation can be obtained:

$$\begin{cases} \dot{\hat{x}}(t) = A\hat{x}(t) + Bu(t) + L\left[y_f(t) - \hat{y}(t)\right] \\ \hat{y}(t) = C\hat{x}(t) \\ r(t) = y_f(t) - \hat{y}(t) \end{cases}, \tag{8}$$

where $\hat{x}$, $\hat{y}$ and r denotes the estimated state, estimated output and residual vector, respectively. The matrices L is an observer gain that is to be designed.

Figure 5 Structure diagram of fault observer

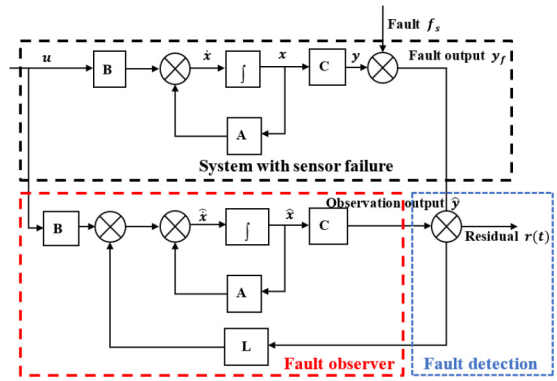

Let $e(t) = x(t) - \hat{x}(t)$ be the state estimation error, it follows from equations (7) and (8) that the error dynamics can be described by:

$$\begin{cases} \dot{e}(t) = (A - LC)e(t) - LF_s f_s(t) + Dd(t) \\ r(t) = Ce(t) + F_s f_s(t) \end{cases}, \tag{9}$$

To facilitate the analysis of the residual robustness performance and fault-sensitive performance, according to the superposition theorem of linear systems, equation (9) is decomposed into the following two subsystems:

$$\begin{cases} \dot{e}_d(t) = (A - LC)e_d(t) + Dd(t) \\ r_d(t) = Ce_d(t) \end{cases}, \tag{10}$$

$$\begin{cases} \dot{e}_f(t) = (A - LC)e_f(t) - LF_s f_s(t) \\ r_f(t) = Ce_f(t) + F_s f_s(t) \end{cases}, \tag{11}$$

where equation (10) represents the estimation error subsystem that is only affected by interference, and equation (11) represents the estimation error subsystem that is only affected by the fault. The two subsystems satisfy:

$$\begin{cases} e(t) = e_d(t) + e_f(t) \\ r(t) = r_d(t) + r_f(t) \end{cases}, \tag{12}$$

Next, the solution theorem of the multi-objective fault observer gain matrix L is given.

Theorem 1 According to the bounded and real lemma, for the equation (7), given scalar $\gamma > 0$ and $\rho > 0$, design the fault observer shown in equation (8), if there are symmetric positive definite matrices P and Q and have a suitable dimensional matrix M, N and the following linear matrix inequality (LMI) inequalities are established at the same time, then the error dynamic equation (9) is gradually stable, while satisfying: $\|G_{r_d d}(s)\|_\infty < \gamma_1, \|G_{r_f f}(s)\|_- > \rho$:

$$\begin{cases} \begin{bmatrix} A^TP + PA - (MC)^T - MC + C^TC & PD \\ * & -\gamma^2 I \end{bmatrix} < 0 \\ \begin{bmatrix} A^TQ + QA - (NC)^T - NC + C^TC & -NF_s - C^TF_s \\ * & F_s{}^TF_s + \rho^2 I \end{bmatrix} < 0 \end{cases}, \tag{13}$$

Proof: Assume that the SBW system has not failed, and only consider that the system has unknown interference inputs. Let $f_s(t) = 0$ and bring it into equation (9) to get equation (10).

$$\dot{V}(e_d) = \dot{e}_d^T P e_d + e_d^T P \dot{e}_d = e_d^T \Big((A - LC)^T P + P(A - LC) \Big) e_d + 2 e_d^T P D d$$

$$\begin{aligned} \mathcal{J} &= \int_0^t r_d{}^T r_d dt - \gamma^2 \int_0^t d^T d dt = \int_0^t \left(r_d{}^T r_d - \gamma^2 d^T d \right) dt \\ &< \int_0^t \Big(r_d{}^T r_d - \gamma^2 d^T d + \dot{V}(e_d) \Big) dt \\ &= \int_0^t \left\{ \begin{bmatrix} e_d \\ d \end{bmatrix}^T \begin{bmatrix} A^T P + PA - (PLC)^T - PLC + C^T C & PD \\ * & -\gamma^2 I \end{bmatrix} \begin{bmatrix} e_d \\ d \end{bmatrix} \right\} < 0 \end{aligned}$$

As $V(e_d) > 0$, it only needs to satisfy:

$$\begin{bmatrix} A^T P + PA - (PLC)^T - PLC + C^T C & PD \\ * & -\gamma^2 I \end{bmatrix} < 0, \tag{14}$$

Because of $\|G_{r_d d}(s)\|_\infty < \gamma \Longleftrightarrow \int_0^t r_d{}^T r_d dt < \gamma^2 \int_0^t d^T d dt$, it is to choose Lyapunov function as $V(e_d) = e_d^T P e_d > 0$, where P is a symmetrically positive matrix:

Similarly, if the SBW system fails, there is no unknown interference input. Let d (t) = 0 and bring it into equation (9) to get equation (11).

Because of $\|G_{r_f f}(s)\|_- > \rho \Longleftrightarrow \int_0^t r_f{}^T r_f dt < \rho^2 \int_0^t f_s{}^T f_s dt$, it is to choose Lyapunov function as $V(e_f) = e_f^T Q e_f > 0$, where Q is symmetrically positive matrix:

$$\dot{V}(e_f) = \dot{e}_f^T Q e_f + e_f^T Q \dot{e}_f = e_f^T \Big((A - LC)^T Q + Q(A - LC) \Big) e_f - 2 e_f^T Q L F_s f_s$$

$$\begin{aligned} \mathcal{J} &= \int_0^t r_f{}^T r_f dt - \rho^2 \int_0^t f_s{}^T f_s dt = \int_0^t \left(r_f{}^T r_f - \rho^2 f_s{}^T f_s \right) dt \\ &< \int_0^t \Big(r_f{}^T r_f - \rho^2 f_s{}^T f_s - \dot{V}(e_f) \Big) dt + V(e_f) \\ &= \int_0^t \left\{ \begin{bmatrix} e_f \\ f_s \end{bmatrix}^T \begin{bmatrix} -(A - LC)^T Q - Q(A - LC) + (QLC)^T - C^T C & QLF_s + C^T F_s \\ * & -F_s{}^T F_s - \rho^2 I \end{bmatrix} \begin{bmatrix} e_f \\ f_s \end{bmatrix} \right\} + V(e_f) > 0 \end{aligned}$$

As $V(e_f) > 0$, it only needs to satisfy:

$$\begin{bmatrix} A^T Q + QA - (NC)^T - NC + C^T C & -NF_s - C^T F_s \\ * & F_s{}^T F_s + \rho^2 I \end{bmatrix} < 0, \tag{15}$$

Let $PL = M$ and $QL = N$ into the equations (14) and (15) to get equation (13), which proof the Theorem 1.

After generating the residual by the fault observer, it is necessary to select an appropriate residual evaluation method to judge whether the system has a fault. Ideally, if the residual is not zero, it indicates that the system has failed. However, in practical applications, the control system is inevitably affected by unmodeled dynamics and parameter changes, so there is a large deviation between the theoretically obtained mathematical model and the actual system, which will invalidate the FD result.

Therefore, this paper chooses the dynamic threshold $\mathcal{J}_{th}$ to compare with the residual evaluation function, so as to reduce the false alarm rate of the fault observer and improve the credibility of the FD result. In this paper, the residual evaluation function when the SBW system contains parameter perturbation, but no sensor failure occurs is taken as the dynamic threshold, and the FD decision logic is:

$$\begin{cases} \mathcal{J}(t) > \mathcal{J}_{th} \Rightarrow AFaultOccurs \\ \mathcal{J}(t) \le \mathcal{J}_{th} \Rightarrow NOFault \end{cases}, \tag{16}$$

where the residual evaluation function is defined as $\mathcal{J}(t) = \|r\|_{RMS} = \sqrt{\frac{1}{T} \int_t^{t+T} r^T(t) r(t) dt}$.

4.2 Multi-objective constraint fault estimator

In this section, an MCFE, as shown in Figure 6, based on the residual information obtained from the fault observer is designed for parameter perturbation and sensor failure in the SBW system. In addition, the gain matrix F and G in the estimator is obtained by using the bounded real theorem and regional pole assignment lemma, and the size, occurrence time and time-varying characteristics of the fault can be determined according to the residual obtained in the previous section.

And the fault estimator is described by the following form:

$$\begin{cases} \dot{\hat{f}}_s(t) = -F(t)\hat{f}_s(t) + Gr(t) \\ Z(t) = \hat{f}_s(t) = E\hat{f}_s(t) \end{cases}, \tag{17}$$

where $\hat{f}_s$ is the estimation value of the sensor fault value f_s. F and G are the gain matrices with appropriate dimensions to be determined later $E(t) = I_r$.

Defining state error $e_x(t) = x(t) - \hat{x}(t)$ and fault estimation error $e_{fs}(t) = f_s(t) - \hat{f}_s(t)$, by the equations (8) and (17), the state estimation error is:

$$\dot{e}_x(t) = (A - LC)e_x(t) - LF_s f_s(t) + Dd(t), \tag{18}$$

Fault estimation error is:

$$\dot{e}_{fs}(t) = \dot{f}_s(t) - GCe_x(t) - Fe_{fs} + (F - GF_s)f_s(t), \tag{19}$$

Let $\bar{e} = \begin{bmatrix} e_x \\ e_{fs} \end{bmatrix}$ and $\bar{d} = \begin{bmatrix} d \\ f_s \\ \dot{f}_s \end{bmatrix}$, the augmented error matrix is obtained as:

$$\begin{cases} \dot{\bar{e}} = \bar{A}\bar{e} + \bar{D}\bar{d} \\ e_{fs} = \bar{C}\bar{e} \end{cases} \tag{20}$$

where $\bar{A} = \begin{bmatrix} A - LC & 0 \\ -GC & -F \end{bmatrix}$, $\bar{D} = \begin{bmatrix} D & -LF_s & 0 \\ 0 & F - GF_s & I \end{bmatrix}$ and $\bar{C} = \begin{bmatrix} 0 & I_r \end{bmatrix}$.

If the extended error dynamic equation (20) converges asymptotically and stably to zero, it is guaranteed that $\hat{x}$ and $\hat{f}_s$ are accurate estimates of state x and fault f_s, respectively. The method of finding the matrices F, G are given below.

Theorem 2 According to the bounded and real lemma, if there is a symmetric matrix $T > 0$ and the following linear matrix inequality LMI is satisfied, the augmented error equation (20) converges to zero asymptotically and steadily. The fault estimator equation (16) can obtain stable state estimation and fault estimation, and the generalized disturbance $\bar{d}(t)$ meets the fault estimation error: $\|G_{e_{fs}\bar{d}}(s)\|_\infty < \gamma_2$

$$\begin{bmatrix} T_1A + A^TT_1 - M_1C - C^TM_1^T & C^TM_2^T & T_1D & -M_1F_s & 0 & 0 \\ * & -M_3 - M_3^T & 0 & M_3 - M_2F_s & T_2 & I \\ * & * & -\gamma I & 0 & 0 & 0 \\ * & * & * & -\gamma I & 0 & 0 \\ * & * & * & * & -\gamma I & 0 \\ * & * & * & * & * & -\gamma I \end{bmatrix} < 0, \tag{21}$$

Proof: refer to Section 2.1 for the proof process.

To further suppress the influence of parameter variation on fault estimation, improve the dynamic characteristics and transient performance of fault estimator, and improve the accuracy of fault estimation, a regional pole assignment lemma is introduced in this paper.

Lemma 1 All the eigenvalues of the state matrix $\bar{A} \in R^{n\times n}$ of a given system are in the vertical bar area $D_{vs}(\lambda \in C : h_1 < \mathrm{Re}(\lambda) < h_2)$, then the system is D stable and only if there is a symmetric positive matrix T satisfying the following matrix inequality:

$$\begin{bmatrix} 2h_1T - (T\bar{A} + \bar{A}^TT) & 0 \\ * & (T\bar{A} + \bar{A}^TT) - 2h_2T \end{bmatrix} < 0, \tag{22}$$

Substitute $T = diag(T_1, T_2)$ into the above formula.

$$\begin{bmatrix} 2h_1T_1 - T_1A - A^TT_1 + M_1C + C^TM_1^T & C^TM_2^T & 0 & 0 \\ * & 2h_1T_2 + M_3 + M_3^T & 0 & 0 \\ * & * & T_1A + A^TT_1 - M_1C - C^TM_1^T - 2h_2T_1 & -C^TM_2^T \\ * & * & * & -M_3 - M_3^T - 2h_2T_2 \end{bmatrix} < 0, \tag{23}$$

Figure 6 Structure diagram of fault estimator

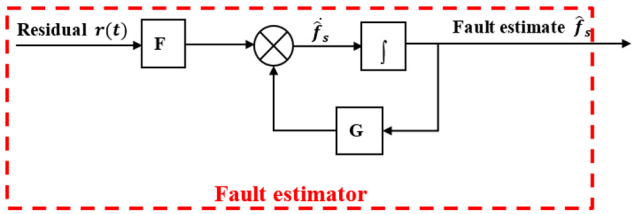

Theorem 2 and Lemma 1 give the design method of the MCFE. Next, we discuss the existence conditions of the MCFE (17).

Theorem 3 Let *rank* $(A) = n$, *rank* $(C) = m$ and *rank* $(F) = r$, then the sufficient and necessary conditions for the existence of the fault estimator (17) are:

$$rank\left(\begin{bmatrix} A-\lambda I_n & 0 \\ 0 & -F-\lambda I_r \\ C & 0 \end{bmatrix}\right) = n+r, \forall s \in \mathbb{C}, \mathrm{Re}(s) \geq 0 \tag{24}$$

Proof: As $rank\left(\begin{bmatrix} C \\ A-\lambda_i I \end{bmatrix}\right) = n$, where λ_i is all the eigenvalues of the system matrix A, (A, C) can be observed.

Rewrite equation (19) as:

$$\begin{cases} \dot{\bar{e}} = (\tilde{A} - \tilde{L}\tilde{C})\bar{e} + \overline{D}\bar{d} \\ e_{fs} = \overline{C}\bar{e} \end{cases}, \tag{25}$$

where $\tilde{A} = \begin{bmatrix} A & 0 \\ 0 & -F \end{bmatrix}$, $\tilde{L} = \begin{bmatrix} L \\ G \end{bmatrix}$, $\tilde{C} = \begin{bmatrix} C & 0 \end{bmatrix}$, $\overline{D} = \begin{bmatrix} D & -LF_s & 0 \\ 0 & F-GF_s & I \end{bmatrix}$ and $\overline{C} = \begin{bmatrix} 0 & I_r \end{bmatrix}$.

According to the linear system theory, we can obtain the sufficient and necessary condition of equation (23) that $(\tilde{A}, \tilde{C})$ is observable, that is:

$$rank\left(\begin{bmatrix} \tilde{A}-\lambda I_{n+r} \\ \tilde{C} \end{bmatrix}\right) = n+r, \forall s \in \mathbb{C}, \mathrm{Re}(s) \geq 0 \tag{26}$$

Substitute $\tilde{A} = \begin{bmatrix} A & 0 \\ 0 & -F \end{bmatrix}, \tilde{C} = \begin{bmatrix} C & 0 \end{bmatrix}$ into the above formula:

$$\begin{aligned} rank\left(\begin{bmatrix} \tilde{A}-\lambda I_{n+r} \\ \tilde{C} \end{bmatrix}\right) &= rank\left(\begin{bmatrix} A-\lambda I_n & 0 \\ 0 & -F-\lambda I_r \\ C & 0 \end{bmatrix}\right) = rank\left(\begin{bmatrix} A-\lambda I_n & 0 \\ C & 0 \\ 0 & -F-\lambda I_r \end{bmatrix}\right) \\ &= rank\left(\begin{bmatrix} A-\lambda I_n & 0 \\ C & 0 \end{bmatrix}\right) + rank\left(\begin{bmatrix} 0 & -F-\lambda I_r \end{bmatrix}\right) \end{aligned} \tag{27}$$

It can be seen from the above that (A, C) is observable, so $rank\left(\begin{bmatrix} A-\lambda I_n & 0 \\ C & 0 \end{bmatrix}\right) = n$ and *rank* $(F) = r$ from the meaning of the question, it is easy to get *rank* $([0\ -F-\lambda I,]) = r$, which is proved.

4.3 Fault reconstructor

When the sensor fails, it can be seen from Section 4.1 that the fault output of the SBW system satisfies:

$$y_f = y + f_s \tag{28}$$

where y, f_s and y_f are sensor fault-free output, sensor fault value and the fault sensor output, respectively.y can be measured by the sensor after the failure of the sensor. If the values of f_s and $\hat{f}_s$ are approximately equal, then the value without failure of the sensor can be obtained through equation (28).

Using the above ideas and based on the sensor fault estimated value $\hat{f}_s$ obtained by the MCFE designed in Section 4.2 and the fault vector F_s obtained in Section 3.2, the fault reconstructor shown in Figure 7 is designed for fault sensor reconstruction, making the SBW system can still guarantee the basic steering function in the event of sensors failure, and maintain the driving stability and safety, and the reconstructor is designed as:

$$y_{ft}(t) = y_f(t) - F_s\hat{f}_s(t) = y_f(t) - \begin{bmatrix} 0 & 1 & 0 & 0 & 0 \\ 0 & 0 & 1 & 0 & 0 \\ 0 & 0 & 0 & 0 & 1 \end{bmatrix}\hat{f}_s(t), \tag{29}$$

where y_f, $F_s\hat{f}_s$ and y_{ft} are the fault sensor output, fault switching matrix, value of fault estimation and fault-tolerant output, respectively.

Keeping the proportion integration differentiation (PID) controller structure unchanged, switching y_{ft} to the feedback

Figure 7 Schematic diagram of reconstructor

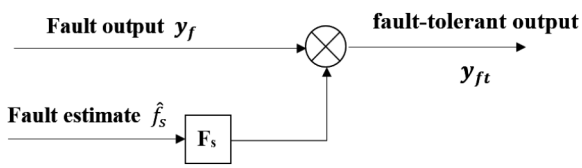

loop of the PID controller can make the SBW system with sensor fault still have steering characteristics close to that of the no-fault SBW system, thus achieving the purpose of fault-tolerant control.

5. Numerical analysis

To demonstrate the effectiveness of the FD, fault estimation and fault-tolerant control strategies are proposed considering parameter perturbation and sensors fault in the SBW system. The simulation environment is set as follows.

- It is assumed that the damping coefficient of the front wheels and steering mechanism on the steering shaft, the damping coefficient of the motor shaft and the perturbation amount of the front wheel deflection stiffness parameter are set within 10% (Huang *et al.*, 2017).
- This article considers that a single sensor has a mixed failure, and multiple sensors have a simultaneous failure. The failure is set as described in Table 1 for simulation verification.
- Set the vehicle speed v_x = 15 m/s, given the target steering wheel angle as shown in Figure 8. The main parameters in the simulation of this paper are shown in Table 2. Under the matrix and laboratory (MATLAB)/Simulink environment, the PID control module, fault setting module, FD module, fault estimation module and fault tolerance control module of the SBW system are established, respectively, to analyze the timeliness and accuracy of FD, the accuracy of fault estimation and the effect of fault-tolerant control.

Table 1 Fault description in details

Fault types	Fault behavior
Continuous deviation-gain failure	Rotation angle sensor deviation fault after 6 s and signal interruption after 9 s
Simultaneous gain-stuck failure	The yaw rate sensor has a gain failure of Δ_1 = 0.3 at t = 9 s, and the rotation angle sensor is lock
Simultaneous interruption-gain failure	Lateral acceleration sensor interrupt fault at t = 5 s, and rotation angle sensor gain fault with Δ_2 = 0.4 at the same time

5.1 Results of fault detection

Using the method in Section 2.1 to design the fault observer, and the mincx command to solve equation (18) can obtain γ_1= 5.273 * 10–4, ρ = 0.4979, as well as the optimal observer feedback gain matrix L as:

$$L = \begin{bmatrix} 1199.30 & 7.98898 \times 10^{-7} & -1.22795 \times 10^{-4} & -150568 & -1.79442 \times 10^{-5} \\ 15152.3 & 1.05084 \times 10^{-5} & -1.69501 \times 10^{-3} & -186578 & -2.48836 \times 10^{-4} \\ 52.5015 & -5.02841 \times 10^{-10} & -4.25239 \times 10^{-8} & -10590 & -7.22559 \times 10^{-9} \\ 3.08463 \times 10^{10} & -0.0184117 & -316.691 & -6.13696 \times 10^{12} & -48.8070 \\ -157.260 & 1.58503 \times 10^{-9} & 1.50850 \times 10^{-7} & 31721 & 2.53699 \times 10^{-8} \\ 1.09552 \times 10^{7} & 1.78152 \times 10^{-4} & 0.0727597 & -1.51664 \times 10^{9} & 1.14525 \times 10^{-2} \\ -2.17262 \times 10^{10} & 0.0464384 & -21.1417 & -2.34267 \times 10^{11} & -3.24072 \end{bmatrix}$$

Substituting the matrix L into the FD observer can obtain the FD results shown in Figures 9–11.

As shown in Figure 9, for the FD of the continuous deviation-gain failure of rotation angle sensor, when there is parameter perturbation and sensor failure in the SBW system, the residual norm exceeds the diagnostic threshold at about 5 s, indicating that a sensor failure has occurred in the system at this time.

As shown in Figure 10, for the FD results of the simultaneous gain-stuck fault of two sensors, it can be seen that the norm of the residual is lower than the diagnostic threshold between 0 s–9 s and the norm of the residual signal exceeds the FD threshold at about 9.1 s. It indicates that the system has a sensor failure at this time, but it cannot be known, which sensor has failed. The norm of the residual does not exceed the diagnostic threshold at 9 s because there is an error in the fitting of the generated residual curve, which leads to FD false alarms; however, the overall FD performance is satisfactory.

As shown in Figure 11, for the FD result of the simultaneous interruption of the two sensors-gain fault, it can be observed that the norm of the residual exceeds the FD threshold at about 5 s, indicating that the system is faulty. However, the test results also cannot indicate what type of fault occurred in which sensor.

From the above simulation results, it can be concluded that the designed fault observer can detect a fault, when they occur

Figure 8 Angular curve of steering wheel

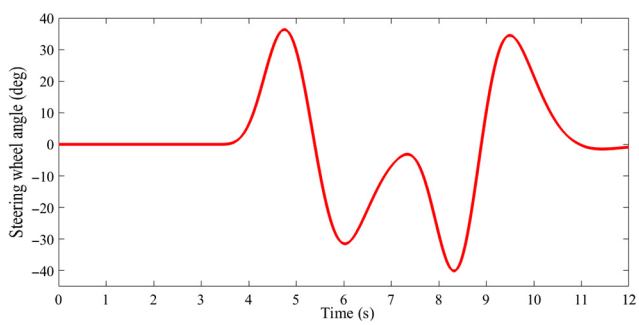

Table 2 Parameters of SBW model

Parameters	Symbols	Values
Body mass	m	1,270 kg
Body roll moment of inertia	Iz	1,537 kg.m^2
Distance from mass center to front wheel	a	1.015 m
Distance from mass center to rear wheel	b	1.895 m
Front wheel cornering stiffness	K_f	135,000 N/rad
Rear wheel cornering stiffness	K_r	175,000 N/rad
Pneumatic trail	t_p	0.006 m
Mechanical trail	t_m	0.014 m
Armature inductance	L	0.003 H
Armature resistance	R	0.034 Ω
Motor torque coefficient	K_t	0.086 N.m/A
Counter electromotive force coefficient	K_e	0.009 V.s/rad
Motor stiffness coefficient	K_m	130 N.m/rad
Motor rotary inertia	J_m	0.006 Kg/m^2
Motor damping	B_m	0.1 N.m.s/rad
Steering tube rotary inertia	J_c	0.01 Kg/m^2
Steering tube damping	J_c	0.3 N.m.s/rad
Steering tube stiffness coefficient	K_c	0.5 N.m/rad
Motor speed-reducing device transmission ratio	G_m	18
Steering ratio	G_1	15.5

for different time periods of a single sensor and multiple sensors simultaneously appearing different types of fault. However, it cannot determine the type of fault, nor can it determine, which sensor is faulty. The multi-objective constraint fault estimator can solve this problem, to further estimate the size and time-varying characteristics of the fault.

5.2 Results of fault estimation

The method in Section 2.2 was used to design the MCFE, and the narrow strip region was selected as $-100 < Re(\lambda) < -10$. In MATLAB, mincx command was used to solve equations (26) and (28) to obtain $\gamma_2 = 0.0105$, and the optimal estimator gain matrices F and G are:

$$F = \begin{bmatrix} 97.79 & 8.41 \times 10^{-6} & -5.37 \times 10^{-5} \\ 8.43 \times 10^{-6} & 97.63 & -0.02 \\ -5.37 \times 10^{-5} & -0.02 & 97.79 \end{bmatrix},$$

$$G = \begin{bmatrix} -1198.17 & 97.79 & -8.60 \times 10^{-6} & 0.18 & -5.38 \times 10^{-5} \\ -1.13 \times 10^{5} & 8.45 \times 10^{-6} & 97.41 & 6.23 & -0.06 \\ -1.91 \times 10^{4} & -5.35 \times 10^{-5} & -0.06 & 0.70 & 97.78 \end{bmatrix}.$$

To show that the MCFE can provide better estimation performance than the fast-adaptive fault estimation observer, the simulation calculation of the fast-adaptive fault estimation observer (Olfa *et al.*, 2015) design is also given below. The LMI toolbox solves the linear matrix inequality to obtain $\gamma^* = 8.266 * 10^{-4}$, the observer gain matrix L and the fault estimation gain G are:

$$L = \begin{bmatrix} 3.91 \times 10^{6} & 1.39 \times 10^{5} & -1.77 \times 10^{4} & -2.03 \times 10^{7} & 1.10 \times 10^{5} \\ 5.32 \times 10^{7} & 1.88 \times 10^{6} & -2.40 \times 10^{5} & -2.76 \times 10^{8} & 1.49 \times 10^{6} \\ 7.02 \times 10^{9} & 2.49 \times 10^{8} & -3.17 \times 10^{7} & -3.63 \times 10^{10} & 1.97 \times 10^{8} \\ 2.97 \times 10^{11} & 1.05 \times 10^{10} & -1.34 \times 10^{9} & -1.83 \times 10^{12} & 8.32 \times 10^{9} \\ -1186.96 & -41.50 & 5.27 & 1.35 \times 10^{5} & -32.83 \\ 6.30 \times 10^{9} & 2.23 \times 10^{8} & -2.84 \times 10^{7} & -3.27 \times 10^{10} & 1.77 \times 10^{8} \\ 4.40 \times 10^{11} & 1.58 \times 10^{10} & -2.01 \times 10^{9} & -2.31 \times 10^{12} & 1.25 \times 10^{10} \end{bmatrix}$$

$$G = \begin{bmatrix} -5.36 \times 10^{7} & 1.18 \times 10^{4} & -2.30 \times 10^{5} & -7136.16 & -9.45 \times 10^{4} \\ 9.19 \times 10^{8} & 3.42 \times 10^{7} & -4.14 \times 10^{6} & 1.46 \times 10^{6} & 2.71 \times 10^{7} \\ 9.41 \times 10^{7} & 5.33 \times 10^{6} & -8.35 \times 10^{5} & 1.89 \times 10^{5} & 4.15 \times 10^{6} \end{bmatrix}.$$

Substituting the above-obtained matrices F and G into the MCFE, and L and G into the fast adaptive fault estimation observer, the fault estimation results can be obtained in Figures 12–21.

As shown in Figure 12, for the estimation results of continuous deviation-gain fault of rotation angle sensor, it can be seen that the multi-objective constraint fault estimator can accurately estimate the fault value as 0, when the rotation angle sensor does not fail during 0 s ∼ 5 s. When the rotation angle sensor has a constant deviation fault after 5 s, the output of the sensor is always about 10 degrees higher than the real value. In addition, the gain fault occurs after 7 s, and the fault estimation curve can accurately approximate the real fault from the time when the fault occurs. However, the adaptive fault estimation method has obvious overshoot in 4 s ∼7 s, and obvious oscillation in 7 s ∼7.5 s. Although the phases of the fault setting curve and the fault estimation curve are the same in 7 s ∼12 s, the amplitudes at the peaks and troughs are significantly different.

Figure 9 Fault detection results of the rotation angle sensor

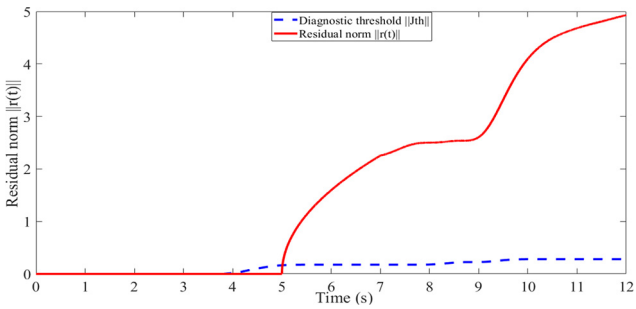

Figure 10 Results of simultaneous gain-stuck detection of two sensors

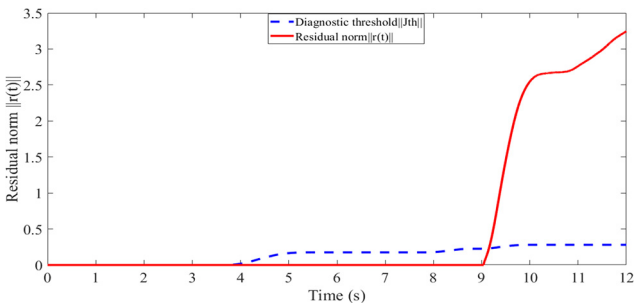

Figure 11 Results of two sensors interrupted at the same time-gain fault detection

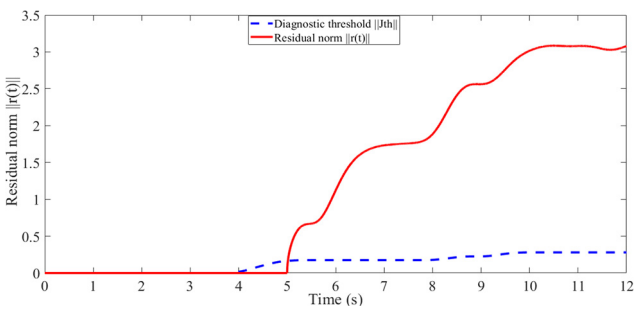

Figure 12 Fault estimation curve of the rotation angle sensor

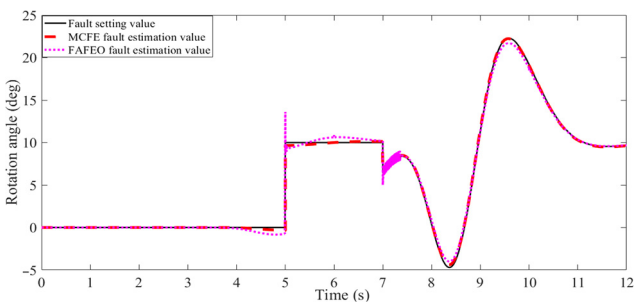

As shown in Figure 13, the error of the fault estimation error is large when the fault occurs. It is because the estimator needs a reaction time to adapt to this sudden fault, and the fault estimation error at all other times is less than 0.7 degrees.

Figure 13 Fault estimation error curve of the rotation angle sensor by estimation method in this paper

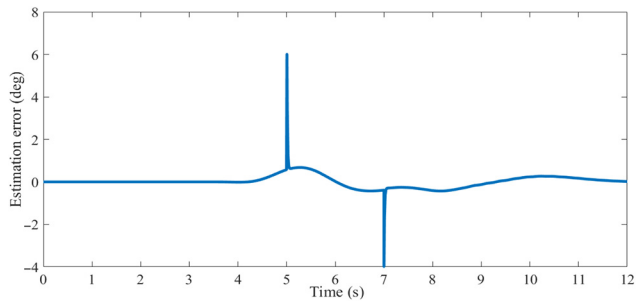

Figure 14 Fault estimation curve of the yaw rate sensor

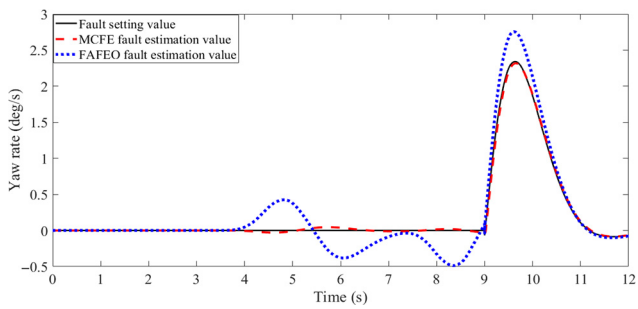

Figure 15 Fault estimation error curve of the yaw rate sensor by estimation method in this paper

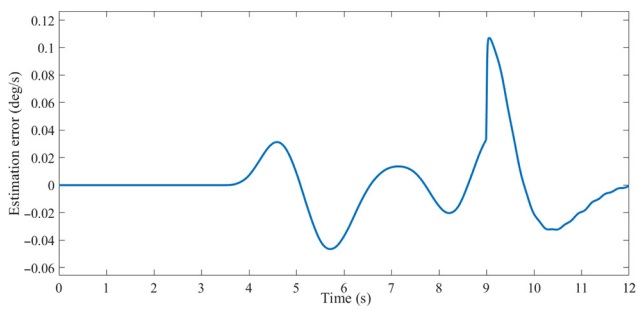

Figure 16 Fault estimation curve of the rotation angle sensor

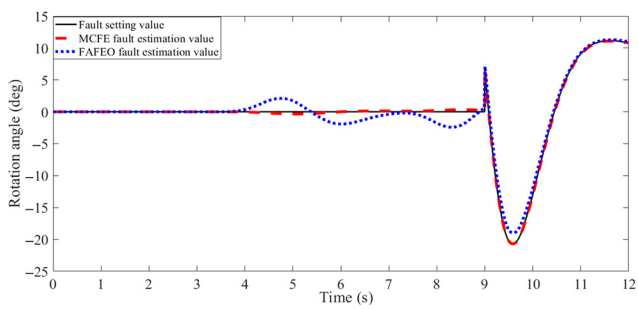

Figure 17 Fault estimation error curve of the rotation angle sensor by estimation method in this paper

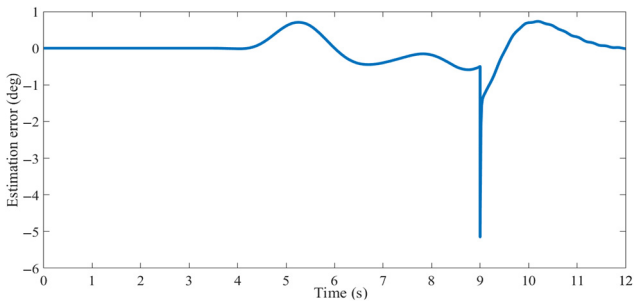

Figure 18 Fault estimation curve of the lateral acceleration sensor

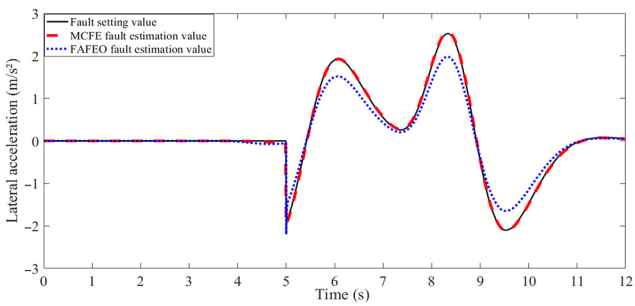

Figure 19 Fault estimation error curve of the lateral acceleration sensor by estimation method in this paper

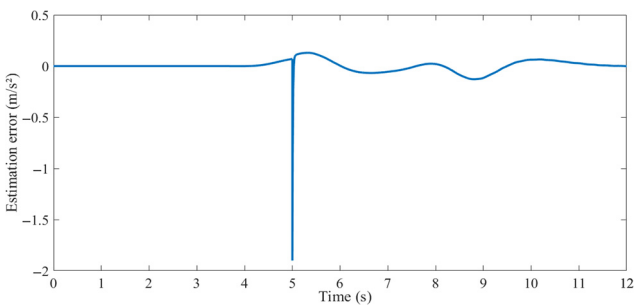

Figure 20 Fault estimation curve of the rotation angle sensor

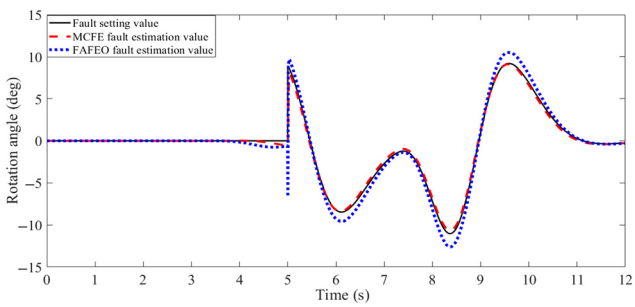

Figure 21 Fault estimation error curve of the rotation angle sensor by estimation method in this paper

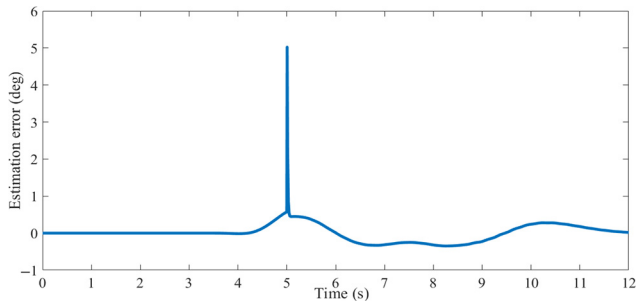

The fault estimation results of the simultaneous gain-stuck fault of two sensors are shown in Figures 14–17.

As demonstrated from Figures 14 and 16, when the yaw rate sensor and the rotation angle sensor have not failed from 0 s to 9 s, the fault estimator can accurately estimate the fault value as 0. When the yaw rate sensor and rotation angle sensor fail simultaneously after 9 s, the yaw rate sensor output is always 0.3 times greater than the true value and the rotation angle sensor output becomes a fixed value from the moment of the failure, and the fault estimation value curve can accurately approximate the real fault from the moment of the fault. However, the adaptive fault estimation algorithm has obvious oscillations from 4 s to 9 s. Although the phases of the fault setting curve and the fault estimation curve are the same between 9 s and 12 s, the amount of overshoot is large at the peak and valley.

As presented in Figures 15 and 17, the fault estimator needs reaction time to adapt to this type of failure, resulting in a spike in the estimation error at 9 s. At other times, the maximum estimation error of the yaw rate and rotation angle are 0.108 deg/s and 0.4 degrees, respectively.

The fault estimation results of the simultaneous interruption-gain fault of two sensors are shown in Figures 18–21.

As shown in Figures 18 and 20, when the lateral acceleration sensor and rotation angle sensor have not failed from 0 s to 5 s, the fault estimator can accurately estimate the fault value as 0. When the lateral acceleration sensor and the rotation angle sensor fail simultaneously after 5 s, the actual output of the lateral acceleration sensor becomes 0, the output of the rotation angle sensor is always 0.3 times more than the true value, and the fault estimation value curve can accurately approximate the real fault from the moment of the fault. However, the adaptive fault estimation algorithm has different amplitudes at the peaks and valleys, for the fault setting curve and the fault estimation curve from the moment of the fault.

As shown in Figures 19 and 21, the fault estimation error is large at 5 s because the estimator needs time to adapt to this type of fault. The peak value of the fault estimation error of the lateral acceleration at the remaining time does not exceed 0.04 m/s^2. In addition, the peak value of the fault estimation error of the rotation angle of the pinion shaft does not exceed 0.4 degrees at the other moments.

From the above fault estimation results, the MCFE designed has strong robustness to system parameter perturbation, and can effectively suppress the influence of system parameter

perturbation on sensor fault estimation results. The fault estimation curve obtained by the multi-objective constraint fault estimator can accurately approximate the real fault from the moment of the fault, with an accuracy rate of up to 98%, which verifies the effectiveness of the fault estimation algorithm designed in this paper.

The comparison of the above fault estimation results also reflects the limitations of the method designed in (Olfa *et al.*, 2015). Due to the error between the adaptive fault observer and the system output, the coupling effect of fault estimation error, state estimation error and the change of adaptive parameters, the gain matrix of the fault is changed, which causes the oscillation of the fault estimation results and a long convergence time.

Comprehensive FD and fault estimation results, when there is parameter perturbation in the SBW system, when a single sensor or multiple sensors have gain, deviation or stuck faults, the fault observer designed in this paper can detect the time when the sensor fails. The fault estimator can accurately estimate the fault amplitude and time-varying characteristics, and the error of fault estimation is generally small, which lays a foundation for the next step of fault-tolerant control.

5.3 Fault-tolerant control results

As shown in Figures 22–24, the comparison curves are presented for the actual sensor output, fault-tolerant control output and fault output under continuous deviation-gain failure, simultaneous gain-stuck failure and simultaneous interruption-gain failure. In the figure, the fault-free output refers to the value when the sensor has not failed, which is represented by a solid black line. The fault-tolerant control outputs refers to the value when the SBW system sensor starts fault-tolerant control after a fault occurrence at time t, which is represented by a red dot line. The fault output refers to the value after a fault occurrence, which is represented by a blue dotted line.

As can be seen from Figure 22, when the rotation angle sensor has no fault from 0 s to 5 s, the actual output, fault-tolerant control output and fault output values are all the same. When a deviation fault occurs after 5 s, the angle of the pinion shaft is always 10 degrees higher than that of the true output. When a gain fault occurs after 7 s, the output of the rotation angle sensor is 0.4 times the normal output, and the peak value of the angle error reaches 32 degrees. When the fault-tolerant

Figure 22 Continuous deviation-gain fault tolerant performance before and after comparison curves

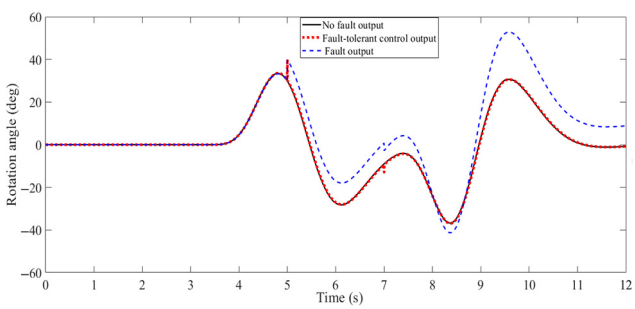

Figure 23 Simultaneous gain-stuck fault tolerant performance before and after comparison curves

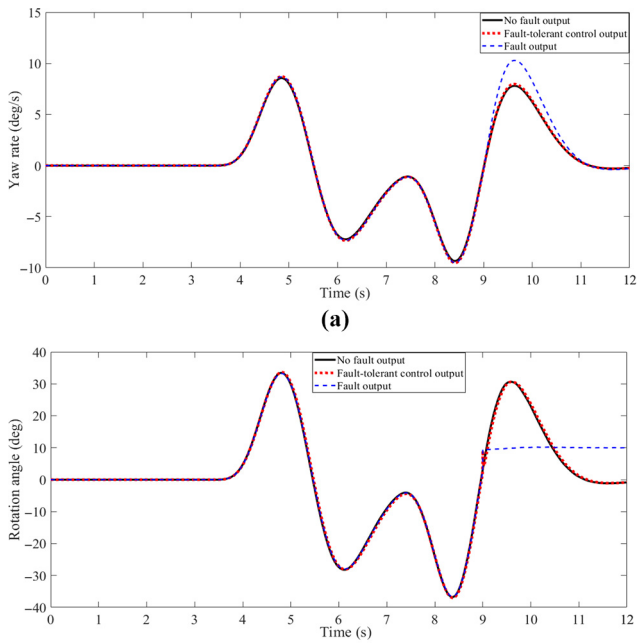

Notes: (a) Performance comparison of the yaw rate sensor before and after fault tolerance; (b) performance comparison of the rotation angle sensor before and after fault tolerance

Figure 24 Simultaneous interruption-gain fault tolerant performance before and after comparison curves

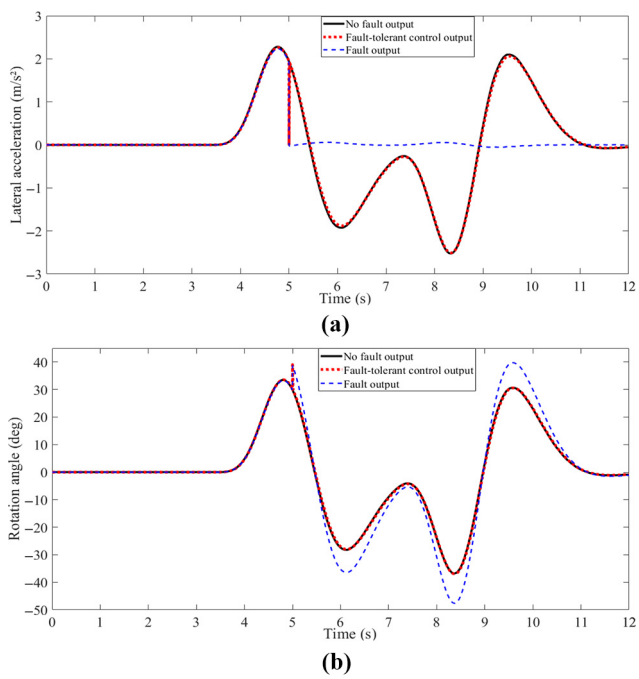

Notes: (a) Performance comparison of the lateral acceleration sensor before and after fault tolerance; (b) performance comparison of the rotation angle sensor before and after fault tolerance

control is started, the output of the fault-tolerant control is consistent with the output of the fault-free SBW system.

As can be seen from Figure 23, when the yaw rate sensor and the rotation angle sensor have not failed from 0 s to 9 s, the actual output, fault-tolerant control output and fault output values are all the same. When the yaw rate sensor has a gain failure after 9 s, the yaw rate error peak value reaches 10 deg/s. At the same time, when the rotation angle sensor is stuck, the output of the rotation angle sensor remains at 10 degrees. When the fault-tolerant control is started, the output of the fault-tolerant control is consistent with the output of the fault-free SBW steering system. It can be seen that fault-tolerant control can significantly reduce the impact of faults on the performance of the SBW system, and restore the performance of the SBW system, to be close to that of the fault-free SBW system.

As can be seen from Figure 24, when the lateral acceleration sensor and the rotation angle sensor have not failed from 0 s to 5 s, the actual output, fault-tolerant control output and fault output values are all the same. When the signal of the lateral acceleration sensor is interrupted after 5 s, the output of the lateral acceleration sensor is always 0, and the peak value of the lateral acceleration error reaches 2.3 m/s^2. At the same time, when the pinion shaft rotation angle sensor has a gain failure, the peak angle error of the pinion shaft reaches 18 degrees. When the fault-tolerant control is started, the output of the fault-tolerant control is consistent with the output of the fault-free SBW system. It can be seen that fault-tolerant control can significantly reduce the impact of faults on the performance of the SBW steering system, and restore the performance of the SBW system to be close to that of the fault-free SBW system.

The above simulation results show that when a single sensor of the SBW system has different faults at different times and multiple sensors fail at the same time, the steering performance of the SBW system will be affected to varying degrees. The fault observer designed in this paper can detect the fault of the sensor more accurately. The multi-objective constraint fault estimator can estimate the fault amplitude of the sensor more accurately when the sensor fails, and the overall error of the fault estimation is smaller. The fault-tolerant control algorithm designed based on the fault estimation information can restore the steering performance of the SBW system to be close to the performance of the fault-free SBW system when the sensor fails. Therefore, it is verified about the effectiveness and feasibility for the fault-tolerant control strategy proposed in this paper.

6. Conclusions

This paper proposes a design method of MCFE, to deal with sensor faults of SBW systems under parameter uncertainties. The residual can be correspondingly obtained by the fault observer to be used as the control input. Therefore, an active fault-tolerant control framework that integrates the fault observer, fault estimator and fault reconstructor is designed to process the rotation angle sensor fault of the SBW system under parameter disturbance.

First, an SBW system model with parameter perturbation and sensor failure is established, and a multi-objective $H\_/H\infty$ fault observer is designed based on the established model. Second, based on the residuals obtained by the fault observer, a fault estimator is designed using bounded real lemma and regional pole configuration to estimate the amplitude and time-varying characteristics of the faulty sensor, and the existence condition of the fault estimation observer is given. Third, a fault-tolerant algorithm is designed based on the sensor fault estimate and fault output. Finally, numerical analysis is carried out to verify the proposed method.

The analyzed results validated that the designed fault observer can accurately and timely diagnose the faults of the sensors of the SBW system, when different types of faults occur in the sensors of the SBW system. The designed MCFE can accurately estimate the sensor fault size and time-varying characteristics, and is robust to parameter perturbation; and the fault-tolerant control strategy can make the SBW system with sensors faulty close to the faultless SBW system. Moreover, the steering characteristics of the system can meet the basic requirements of the wire control system, in which the feasibility and effectiveness are fully verified while applying the active fault-tolerant control framework to the SBW system.

References

Anwar, S. and Niu, W.A. (2010), "Nonlinear observer based analytical redundancy for predictive fault tolerant control of a steer-by-wire system", *2010 IEEE International Conference on Industrial Technology, Vina del Mar, Chile*, pp. 321-334.

Aouaouda, S., Chadli, M., Shi, P. and Karimi, H.R. (2015), "Discrete-time H_/H∞ sensor fault detection observer design for nonlinear systems with parameter uncertainty", *International Journal of Robust and Nonlinear Control*, Vol. 25 No. 3, pp. 339-361.

Chen, L. and Patton, R.J. (2017), "A time-domain LPV H_/H∞ fault detection filter", *IFAC-Papers OnLine*, Vol. 50 No. 1, pp. 8600-8605.

Chengwei, T., Changfu, Z., Xiang, W. and Dong, Y. (2010), "Fault-tolerant control of sensors in steer-by-wire vehicle", *Journal of Jilin University (Engineering Science)*, Vol. 40 No. 1, pp. 6-12 (in Chinese).

Chilali, M. and Gahinet, P. (1996), "H∞ design with pole placement constraints: an LMI approach", *IEEE Transactions on Automatic Control*, Vol. 41 No. 3, pp. 358-367.

Dhahri, S., Sellami, A.B. and Hmida, F. (2012), "Robust sensor fault detection and isolation for a steer-by-wire system based on sliding mode observer", *16th IEEE Mediterranean Electrotechnical Conference, Yasmine Hammamet, Tunisia*, pp. 450-454.

Gao, Z., Yang, L., Wang, H. and Li, X. (2017), "Active fault tolerant control of electric power steering system with sensor fault", *Proceedings of the 36th Chinese Control Conference, Dalian, China*, pp. 9630-9636.

Hou, M. and Patton, R.J. (1996), "An LMI approach to H_/H∞ fault detection observers", *UKACC International Conference on Control, Exeter*, pp. 305-310.

Huang, C., Naghdy, F. and Du, H. (2018), "Observer-based fault-tolerant controller for uncertain steer-by-wire systems using the delta operator", *IEEE/ASME Transactions on Mechatronics*, Vol. 23 No. 6, pp. 2587-2598.

Huang, C., Naghdy, F. and Du, H. (2017), "Fault tolerant sliding mode predictive control for uncertain steer-by-wire system", *IEEE Transactions on Cybernetics*, Vol. 49 No. 1, pp. 261-272.

Ito, A. and Yoshikazu, H. (2013), "Design of fault tolerant control system for electric vehicles with steer-by-wire and in-wheel motors", *Advances in Automotive Control, Tokyo, Japan*, pp. 556-561.

Liang, X., Wang, Q., Hu, C. and Dong, C. (2019), "Observer-based H_∞ fault-tolerant attitude control for satellite with actuator and sensor faults", *Aerospace Science and Technology*, Vol. 95, pp. 1-9.

Lu, X., Zhiqiang, F., Zengliang, L. and Renxie, Z. (2017), "Fault diagnosis of steer-by-wire system for unmanned vehicle", *China Mechanical Engineering*, Vol. 28 No. 22, pp. 2689-2694+2700 (in Chinese).

Mi, J., Wang, T. and Lian, X. (2018), "The two-mode control for steer-by-wire system", *Proceedings of the 37th Chinese Control Conference, Wuhan, China*, pp. 7924-7929.

Mortazavizadeh, S.A., Ebrahimi, M., Ghaderi, A. and Hajian, M. (2020), "Fault-tolerant control of steer-by-wire systems under voltage and current sensors faults", *Electrical Engineering*, pp. 1-9.

Olfa, H., Boumedyen, B. and Ahmed, Z. (2015), "On fault tolerant control of mobile robot based on fast adaptive fault estimation", *12th IEEE International Multi-Conference on Systems, Signals & Devices, Mahdia, Tunisia*, pp. 1-6.

Tian, C., Zong, C., He, L. and Dong, Y. (2009), "Fault tolerant control method for steer-by-wire system", *2009 International Conference on Mechatronics and Automation, Changchun, China*, pp. 291-295.

Wada, N., Fujii, K. and Saeki, M. (2013), "Reconfigurable fault-tolerant controller synthesis for a steer-by-wire vehicle using independently driven wheels", *Vehicle System Dynamics*, Vol. 51 No. 9, pp. 1438-1465.

Waraus, D. (2009), "Steer-by-wire system based on FlexRay protocol", *IEEE Transactions on Applied Electronics, Pilsen, Czech Republic*, pp. 269-272.

Wenhan, Z., Zhenhua, W., Tarek, R., Ye, W. and Yi, S. (2020), "A state augmentation approach to interval fault estimation for descriptor systems", *European Journal of Control*, Vol. 51, pp. 19-29.

Xiao, L., Meng, Z., Huang, X. and Ma, L. (2019), "Adaptive observer based fault tolerant control for aircraft engine with sensors and actuators faults", *Proceedings of the 38th Chinese Control Conference, Guangzhou, China*, pp. 4885-4889.

Yang, J., Zhu, F., Wang, X. and Bu, X. (2015), "Robust sliding-mode observer-based sensor fault estimation, actuator fault detection and isolation for uncertain nonlinear systems", *International Journal of Control, Automation and Systems*, Vol. 13 No. 5, pp. 1037-1046.

Yang, J., Hamelin, F., Apkarian, P. and Sauter, D. (2013), "Mixed H_/H∞ fault detection observer design for multi model systems via nonsmooth optimization approach", *2013 Conference on Control and Fault-Tolerant Systems, Nice, France*, pp. 164-171.

Zhang, J., Swain, A.K. and Nguang, S.K. (2013), "Robust sensor fault estimation scheme for satellite attitude control systems", *Journal of the Franklin Institute*, Vol. 350 No. 9, pp. 2581-2604.

Zhang, H. and Zhao, W. (2016), "Two-way H∞ control method with a fault-tolerant module for steer-by-wire system", *Proceedings of the Institution of Mechanical Engineers, Part C: Journal of Mechanical Engineering Science*, Vol. 232 No. 1, pp. 42-56.

Zhou, M., Wang, Z., Shen, Y. and Shen, M. (2017), "H_/H∞ fault detection observer design in finite-frequency domain for lipschitz non-linear systems", *IET Control Theory & Applications*, Vol. 11 No. 14, pp. 2361-2369.

Further reading

Balachandran, A. and Gerdes, J.C. (2013), "Artificial steering feel design for steer-by-wire vehicles", *IFAC Proceedings Volumes*, Vol. 46 No. 21, pp. 404-409.

Corresponding author

Rencheng Zheng can be contacted at: rencheng.zheng@tju.edu.cn